Contact caustics measurements expanded to anisotropic materials

A. BAKIĆ, D. SEMENSKI, S. JECIĆ
University of Zagreb, Faculty of Mechanical Engineering and Naval Architecture, Ivana Lučića 5, 10000
Zagreb, Croatia

Regions with high stress gradients represent critical zones of engineering structures, such as crack tip or vicinity of the contact zone. The optical method of caustics is one of the few experimental methods which provide applicable results in these locations. This method was originally developed for crack-tip measurements of stress intensity factors and J-integral for isotropic and then for anisotropic materials. Subsequently, it was extended to the contact problems, where the size and the shape of caustics are related to the amount and the inclination of loading force. Here, the application of the method of caustics is extended to the analysis of contact problems for mechanically anisotropic materials. This makes the caustics method widely applicable to the analysis of any high stress gradient locations in a structure.

Keywords: caustics, composites, contact

1. Introduction

During the application of the contact force, surfaces of the model are deformed to a convex shape and the reflected light is not homogenous any more; instead, a dark spot surrounded by the concentrated light on its edge (caustics) can be observed on the screen. When non-transparent materials are concerned, it is possible to record caustics only by utilizing the light reflected from the model surface. On the other hand, when transparent materials are concerned, caustics can be formed by the reflecting light from both the front and the rear surface of a model. Since the screen is in front of the model, only a virtual image is obtained. It can be converted into a real image by transferring the light through the focus of a convex lens.

Simulations of the optical effect for the anisotropic materials indicated that the size and the shape of caustic curve depend not only on the loading condition but also on the mechanical material properties. In isotropic materials the shape of the caustics curve is of unique shape for all materials and can be expressed by the epicycloids equation [1], [2].

A plate loaded by cylindrical punch is considered as material model. The illustrative examples for two materials will be shown. A referent isotropic material is Araldit B (E= 3,48 GPa, υ= 0.38) and as anisotropic material uniaxial carbon fibre-reinforced (CFRP131) is used (E_L= 131 GPa, E_T=E_B= 12 GPa, G_{LT}=18 GPa, υ_{LT}= 0.29, υ_{TL}= 0.29,

$\upsilon_{TB}= 0.34$). Uniaxial carbon fibre-reinforced materials are extremely anisotropic materials which is suitable for analyzing how anisotropy effect on the shape of caustics. Another benefit of such material is a small diameter of fibres (up to 10 μm), which makes it applicable for macro-mechanical analysis. Dimensions of the plate specimen are 50x50x3 mm and they are the same for both materials.

2. Theory of contact caustics

For an analytical approach of the optical effect it is necessary to connect model deformations with the load condition. Lekhnitskii [3], among others, provided an explicit solution to this problem for anisotropic materials by using a complex variable under the following assumptions: the material is of linear elastic characteristics, from a macro-mechanical point of view the material is a homogeneous continuum and the model is in a state of plane stress.

These conditions are satisfied for a thin plate of material with general rectilinear anisotropy and one plane of elastic symmetry (*x-y* plane). Therefore, the compliance material matrix, S_{ij}, consist 13 nonzero elastic constants.

The contact problem is described as the action of a force *F* inclined by the angle α on the anisotropic semi-infinite plane (Figure 1). The complex variable is $z_k = x + \mu_k y$, where μ_k are the roots of the characteristic equation

$$S_{11}\mu_k^4 - 2S_{16}\mu_k^3 + \left(2S_{12} + S_{66}\right)\mu_k^2 - 2S_{26}\mu_k + S_{22} = 0 \qquad (1)$$

$$\mu_1 = \alpha_1 + i\beta_1 \ (\beta_1 > 0), \qquad \mu_3 = \bar{\mu}_1,$$

$$\mu_2 = \alpha_2 + i\beta_2 \ (\beta_2 > 0), \qquad \mu_4 = \bar{\mu}_2. \qquad (2)$$

The equation contain information about the mechanical characteristics of the material in the *x* and *y* direction. If the principal axes of orthotropy are arbitrarily rotated regarding to *x-y* coordinates corresponding coefficients S_{mn} should be recalculated before applying to the characteristic equation

$$S_{ij} = a_{im} a_{jn} S_{mn}. \qquad (i, j, m, n = 1, 2, 3, 6) \qquad (3)$$

The stress state can be derived in the following form

$$\sigma_r = -\frac{FS_{11}}{r\,\pi L(\varphi)}\left[(a\sin\varphi + b\cos\varphi)\sin\alpha + ((\beta+\delta)\sin\varphi + a\cos\varphi)\cos\alpha\right],$$

$$\sigma_\varphi = \sigma_{r\varphi} = 0$$

(4)

where,

$$L(\varphi) = S_{11}\cos^4\varphi + 2S_{16}\sin\varphi\cos^3\varphi + (2S_{12} + S_{66})\sin^2\varphi\cos^2\varphi +$$
$$+ 2S_{26}\sin^3\varphi\cos\varphi + S_{22}\sin^4\varphi,$$

(5)

$$a = \alpha_1\beta_2 + \alpha_2\beta_1, \quad b = \left(\alpha_1^2 + \beta_1^2\right)\beta_2 + \left(\alpha_2^2 + \beta_2^2\right)\beta_1$$

(6)

Transversal deformation for the stress state is derived from Hooks low

$$\varepsilon_z = S_{31}\sigma_x + S_{32}\sigma_y + S_{36}\tau_{xy}.$$

(7)

Although all these equation are valuable for general rectilinear anisotropy analytical solution of the caustic curve will be carried out for orthotropic materials. Materials at our disposal are mainly of orthotropic structure and it is possible to find the principal axes of orthotropy: L-longitudinal, T-transversal and B-bitransversal, which is directed across the plate thickness.

2.1 The formation of caustics on the screen

The explanation of the reflection method of caustics to the non-transparent materials starts from the basic principle of the optical low of reflection. The specimens is loaded and illuminated by the concentrated field of light in the zone of high deformation gradients. The light beams were reflected and transferred from the specimen surface to the virtual plane at distance z_0. The result on the screen is a dark spot, surrounded by the concentrated light on its edge. The position of single light at the point P'(x',y') on the screen is defined by the vector $\vec{r}'$, and its corresponding point P(x,y) on the model is defined by the vector $\vec{r}$ (Figure 2).
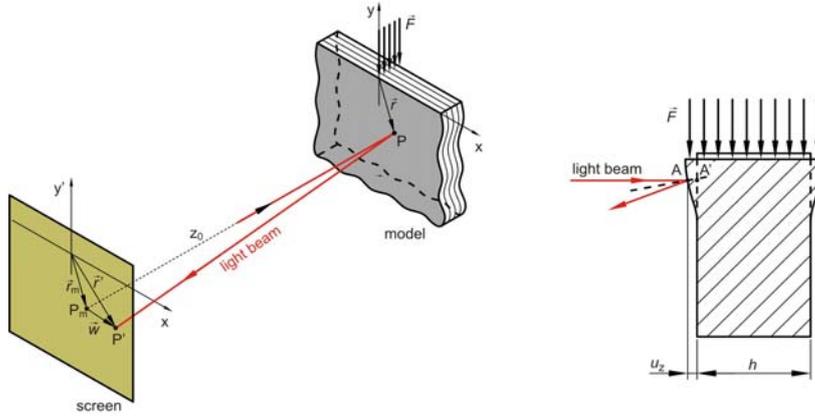
Figure 1. Geometric principle of the beam deflection in the reflecting optical setup

The vectors are related by equations

$$\vec{r}\,' = \vec{r}_m + \vec{w} = m\vec{r} + z_0 grad\,\Delta s , \qquad (8)$$

where m is a magnification factor and Δs is the light beam retardation. Magnification factor depends on modulated light: parallel light $m=1$, convergent light $m<1$ and divergent light $m>1$.

Retardation of the reflected light beam for non-transparent materials is given by a simple equation (Figure 2)

$$\Delta s = s - s' = 2\left|AA'\right| = 2u_z(x,y) = h\varepsilon_z . \qquad (9)$$

where s is the optical path of the light beam for unloaded and s' is optical path for loaded specimen. So, formula (5) transformed to:

$$\vec{r}\,' = \vec{r}_m + w = mr + z_0 h\,grad\,\varepsilon_z , \qquad (10)$$

where

$$grad\,\varepsilon_z = \varepsilon_{z,r}\vec{e}_r + \frac{1}{r}\varepsilon_{z,\phi}\vec{e}_\phi . \qquad (11)$$

Finally, the position of the light beam on the screen is

$$x' = mr\sin\phi - z_0 h\left(\varepsilon_{z,r}\sin\phi + \frac{1}{r}\varepsilon_{z,\phi}\cos\phi\right),$$ (12)

$$y' = -mr\sin\phi - z_0 h\left(-\varepsilon_{z,r}\cos\phi + \frac{1}{r}\varepsilon_{z,\phi}\sin\phi\right).$$ (13)

2.2 Singular caustics curve and initial curve

The singular caustic curve is a highly illuminated edge surrounding the dark spot. The condition of singularity is the Jacobian determinant equals to zero

$$J = \frac{\partial(x',y')}{\partial(r,\varphi)} = x'_{,r}\,y'_{,\varphi} - x'_{,\varphi}\,y'_{,r} = 0.$$ (14)

This function represents the position of the initial curve on the specimen, where the light beams are reflected and projected onto the singular caustic curve. In order to show the solution equation the following function are introduced.

The solution r_0 of the equation (14) leads to six roots: two of them are the pairs of complex conjugate roots, one root is out of the material and has no physical meaning. Only one root is the real and represents the initial curve on the specimen surface [4]
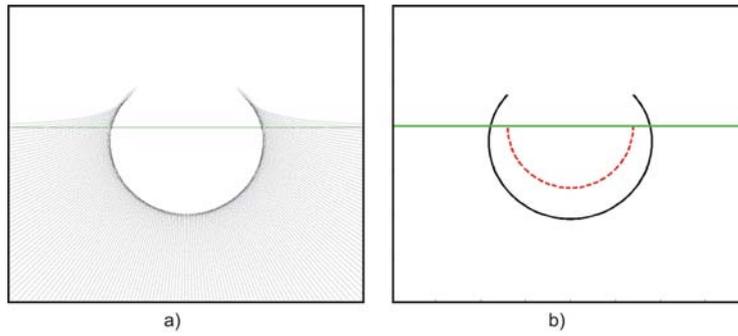

Figure 2. Position of the light beams on the screen a), single caustics curve (solid line)
and initial curve (dash line) b)

Figure 2a shows simulated position of the light beams on the screen while Figure 2b shows singular caustic curve (solid line) and initial curve (dash line).

3. Experiments and results

The optical setup consists of a white light source, lenses, a semi-mirror and a digital camera used as a screen. The thickness of models is 3 mm, which is sufficient for the purpose of avoiding the buckling effect. The surface of Araldit is optically flat and needs no preparation, but the surface of carbon fibre-reinforced composite is textured and should be treated. Here, chemical vapour deposition of an aluminium layer is performed; [5]. The applied aluminium layer has the thickness of approximately 20 microns; therefore, it has no influence on the material strength.

Cause of non-transparent properties of composite material only recording in a reflecting light is considered (Figure 3). Semi-mirror is used to make possible perpendicular path of the light rays onto model surface. Light beam comes from the light source (LS) and passes through the convergent lens (L_1) and semi-mirror (M) prior to illuminates the specimen. Semi-mirror reflects the light on a digital camera (RP) which is used as a screen. Lens (L_2) is optional and it can be convergent ($m<1$), divergent ($m>1$) or it can be left out ($m=1$).
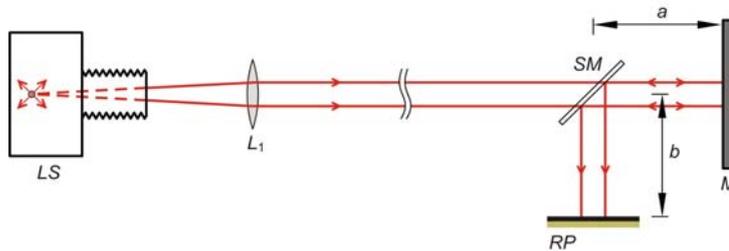

Figure 3. Schematic illustration of the optical setup for recording caustics in the reflecting light.
Light source (LS), lenses (L), semi-mirror (SM), model (M) and reference plane (RP)

Table 1. Parameters of the optical setup

f_{L1}	f_{L2} (divergent lens)	f_{L2} (convergent lens)	x_{L2}	a	b
1000 mm	-600 mm	2000 mm	100 mm	160 mm	100-1200 mm

The optimized values and distances for recording clear image are given in Table 1. Figure 4 shows elements of the optical setup in the laboratory. All elements can be accurately set in optical axis by screws and can be moved along the axis in order to

optimize setup. Large distances between lenses are used to clear the light of unwanted reflections and filter (F) is added to control light intensity on the screen.

Digital camera is set up on the slider which allows continuously changing of z_0 which affect directly on position of initial curve on the specimen.
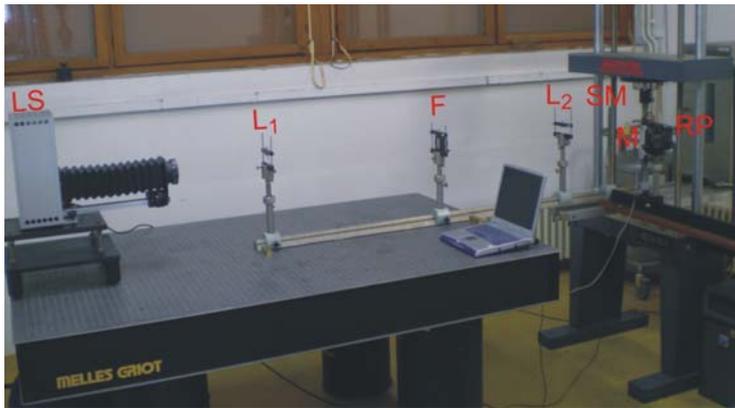

Figure 4. Experimental optical setup

By described optical layout virtual image is obtained on the screen. For obtaining real image it is necessary to add another convergent lens between mirror and digital camera which will invert light through the focus before the screen. Experimental recordings shown that real image is much smaller then virtual one and has no characteristic value to measure.

The bigger one of two caustics shown in Figure 5a is formed on the screen as a reflection from the front surface of the specimen, while the smaller caustics is formed as a reflection from its rear surface. The double effect appears due to birefraction properties of Araldit B because in the case of rear surface reflection light ray should pass through the specimen. Mathematical description of this effect includes not only the surface deformation but also the stress state of a model. Characteristic size of caustics is chosen as y_c which corresponds to radial component of singular caustics curve for $\varphi=0$.

Figure 5b shows the experimentally recorded caustics on the composite material CFRP131 for the case when the fibers are oriented at an angle 45° relative to the direction of the load. The asymmetric optical effect confirms a strong influence of the material orientation on the shape of caustics.

Position of the initial curve on a model depends upon parameter $r_0(\varphi)=r_0(F,m,z_0,S_{ij})$. For the same loading conditions and same specimen, the value of r_0 can still be changed by modifying m (lens L_2) or z_0 (sliding the camera).
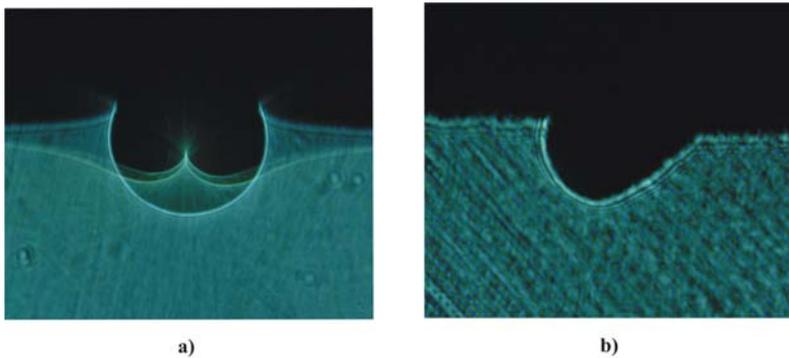

a)   b)

Figure 5. Visual optical effect of the caustics recorded on Araldit B a) and on CFRP131
with fibers orientation at an angle of 45° to the direction of the load b)

Diagram shown on the Figure 6 shows the comparison of analytical and experimental value of characteristic size of caustics. Intensity of contact force was 100 N for Araldit B and 600 N for composite CFRP131. Maximal range of r_0 with presented optical setup was between 1mm and 5 mm. The highest value of r_0 is achieved in convergent light with the large distance z_0.
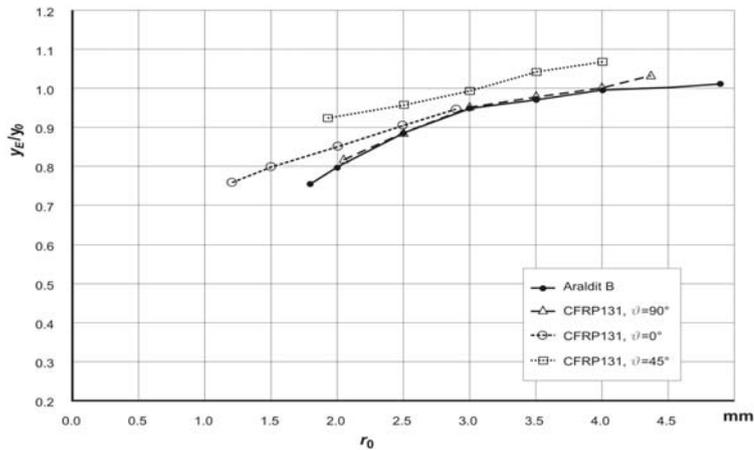

Figure 6. Comparison between experimental and analytical size of caustics for different
position of initial curve and different material properties

3. Conclusion

The simulations of the optical effect and the experiments confirm that for the anisotropic materials size and shape of caustic curve depend not only on the loading condition but also on the mechanical material properties. In isotropic materials the shape of the caustics curve is unique for all materials and can be expressed by the epicycloide.

The obtained results show that significant differences between analytical and experimental approach for small r_0 because analytical model has assumption of elastic material which is not valid for plasticity region near the contact point. Outside this nonlinear zone the results have good agreement but for value of r_0 grater then 5mm size of caustics going down and measuring uncertainty rise up.

The asymmetric optical effect appeared when coordinate axes are not parallel to the principal axes of orthotropy which confirms a strong influence of the material orientation on the shape of caustics.

By varying the input parameters, it is revealed that virtual image is sensitive to the intensity of contact force, while the real image is sensitive to the contact force inclination. Also it is noticed that for anisotropic specimen the real image is small and has no characteristic value to measure, while virtual image is characteristically distinguished for the same load condition.

References
[1] Kalthoff J. F.: *Stress Intensity Factor Determination by Caustics*, Proc. of Int. Conf. on Experimental Stress Analysis, Honolulu-Maui-Hawaii, 1982.
[2] Papadopoulos G. A.:. *Fracture Mechanics: The Experimental Method of Caustics and the Det.-Criterion of Fracture*, Springer-Verlag publisher, Berlin 1992.
[3] Lehnitskii S. G.: *Theory of Elasticity of an Anisotropic Body*, Mir Publishers, Moscow 1950.
[4] Bakić A.:*The method of caustics in contact problems of composite materials (in Croatian)*, PhD thesis, FSB Zagreb, 2009.
[5] Semenski D.: *The application of caustics in fracture mechanics of anisotropic materials (in Croatian)*, PhD thesis, FSB Zagreb, 1995.